

# Optimization and Kinetic Studies of Enzymatic Saccharification of Double-Stage Ozonolysis Pretreated Oil Palm Empty Fruit Bunch for Enhanced Sugar Production

Nur Zahidah Majid<sup>1</sup>, Amnani Shamjuddin<sup>1\*</sup>, Mohd Asmadi<sup>1</sup>, Umi Aisah Asli<sup>1</sup>, Sharifah Nurain Hussain<sup>1</sup>, Riyani Tri Yulianti<sup>1,6</sup>, Nur Hidayah Zainan<sup>2,3</sup>, Nardiah Rizwana Jaafar<sup>3</sup>, Asiah Nusaibah Masri<sup>4,5</sup>, Gwendoline Christophe<sup>7</sup>, Phillipe Michaud<sup>7</sup>

<sup>1</sup>Chemical Reaction Engineering Group (CREG), Faculty of Chemical and Energy Engineering, Universiti Teknologi Malaysia (UTM), 81310 Johor Bahru, Johor, Malaysia.

<sup>2</sup>Centre of Lipid Engineering Applied Research (CLEAR), Faculty of Chemical and Energy Engineering, Universiti Teknologi Malaysia (UTM), 81310 Johor Bahru, Johor, Malaysia.

<sup>3</sup>Department of Bioprocess and Polymer Engineering, Faculty of Chemical and Energy Engineering, Universiti Teknologi Malaysia (UTM), 81310 Johor Bahru, Johor, Malaysia.

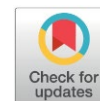
<sup>4</sup>UTM-MPRC Institute for Oil & Gas, Faculty of Chemical and Energy Engineering, Universiti Teknologi Malaysia (UTM), 81310 Johor Bahru, Johor, Malaysia.

<sup>5</sup>Energy Management Group, Faculty of Chemical and Energy Engineering, Universiti Teknologi Malaysia (UTM), 81310 Johor Bahru, Johor, Malaysia

<sup>6</sup>Research Center for Electronics, National Research and Innovation Agency (BRIN), KST Sama'un Samadikun, Jl. Sangkuriang, Bandung, 40135, Indonesia

<sup>7</sup>Université Clermont Auvergne, CNRS, Clermont auvergne INP, Institut Pascal, 63000 Clermont-Ferrand, France.

Received: 30<sup>th</sup> April 2026; Revised: 25<sup>th</sup> June 2026; Accepted: 26<sup>th</sup> June 2026  
Available online: 4<sup>th</sup> July 2026; Published regularly: October 2026



## Abstract

Oil Palm Empty Fruit Bunch (OPEFB), an abundant lignocellulosic biomass in Malaysia, is a promising feedstock for producing Total Reducing Sugar (TRS), although its recalcitrant structure limits enzymatic conversion. This study proposes a novel double-stage ozonolysis pretreatment integrated with intermediate alkaline swelling to enhance cellulose accessibility and saccharification efficiency. Structural modifications were confirmed through compositional analysis, TGA, XRD, FTIR, and SEM. Enzymatic saccharification (ES) was optimized using Response Surface Methodology (RSM) based on a Face-Centered Central Composite Design (FCCCD), evaluating reaction time, biomass loading, and temperature. Analysis of Variance (ANOVA) indicated a significant model ( $R^2 = 0.88$ ), with optimal conditions of 44 h reaction time, 1.8 % w/v biomass loading, and 50 °C temperature, achieving a maximum TRS yield of 42.75%. The double-stage ozonolysis outperformed single-stage and alkaline pretreatments, yielding the highest cellulose enrichment (up to 79 wt%) and improved digestibility. Kinetic analysis revealed a substantial reduction in the Michaelis-Menten constant ( $K_m$ ) from 175.713 to 9.010 mg/mL, indicating enhanced enzyme-substrate affinity. These findings demonstrate a robust and efficient strategy for improving biomass-to-sugar conversion.

Copyright © 2026 by Authors, Published by BCREC Publishing Group. This is an open access article under the CC BY-SA License (<https://creativecommons.org/licenses/by-sa/4.0>).

**Keywords:** Oil palm empty fruit bunch; Biomass pretreatment; Ozonolysis; Optimization; Enzymatic saccharification; Total reducing sugar

**How to Cite:** Abd Majid, N. Z., Shamjuddin, A., Asmadi, M., Asli, U. A., Hussain, S. N., Yulianti, R. T., Zainan, N. H., Jaafar, N. R., Masri, A. N., Christophe, G., Michaud, P. (2026). Optimization and Kinetic Studies of Enzymatic Saccharification of Double-Stage Ozonolysis Pretreated Oil Palm Empty Fruit Bunch for Enhanced Sugar Production. *Bulletin of Chemical Reaction Engineering & Catalysis*, 21 (3), 717-736. (DOI: 10.9767/bcrec.20721)

**Permalink/DOI:** <https://doi.org/10.9767/bcrec.20721>

## 1. Introduction

The current market for biofuels, defined as fuel products obtained from organic substrates, is

dominated by bioethanol, biodiesel, biobutanol and bio-gas, relying on the use of substrates such as sugars, starch, oil crops, agricultural and animal wastes, and lignocellulosic biomass [1]. Oil palm empty fruit bunch (OPEFB) generally consists of three main components: 37.26–63% of

\* Corresponding Authors.

Email: amnani.shamjuddin@utm.my (A. Shamjuddin)

cellulose, 14.6–37% of hemicellulose, and 17–31.7% of lignin [2]. Nevertheless, the recalcitrant structure of the biomass itself, including the biological barrier lignin, significantly limits the conversion of OPEFB into total reducing sugar (TRS), which can be further used to produce biofuels and other value-added biochemicals.

Pretreatment of OPEFB is essential to overcome its inherent recalcitrance, primarily governed by the lignin–carbohydrate complex (LCC), which restricts enzyme accessibility and limits TRS production. Conventional pretreatment methods are broadly categorized as physical, chemical, and biological approaches [3–6]. Physical pretreatment primarily reduces biomass particle size using mechanical processes such as milling or grinding to increase surface area; however, it is generally insufficient to significantly disrupt lignin structures [3]. Chemical pretreatment, particularly alkaline treatment using sodium hydroxide, is more effective in solubilizing lignin and partially removing hemicellulose, thereby enhancing cellulose accessibility [7]. This alkaline treatment induces biomass swelling, reduces cellulose crystallinity, and increases internal surface area and pore volume, thereby enhancing enzymatic accessibility and TRS production [8,9]. Nevertheless, alkaline pretreatment often requires prolonged reaction time, extensive chemical usage, and subsequent washing and neutralization steps, leading to increased operational costs and environmental concerns [10,11]. Biological pretreatment involves the use of enzymes, microbes, or other biological agents, alone or in combination, to convert the biomass into TRS. Biological pretreatment offers a milder alternative but is typically limited by slow reaction rates and lower process efficiency.

In contrast, the ozonolysis process has recently emerged as a promising green pretreatment technology due to its strong oxidative capability, enabling selective lignin degradation under relatively mild conditions without generating toxic by-products [12]. Ozone preferentially attacks the biomass's electron-rich aromatic structures in lignin, effectively disrupting the LCC while largely preserving cellulose integrity [12,13]. Despite these advantages, conventional single-stage ozonolysis pretreatment remains constrained by limited ozone penetration, incomplete delignification and inefficient ozone utilization, particularly in dense biomass matrices. Another limitation is that single-stage ozonolysis may not sufficiently disrupt the LCC, leaving residual lignin that continues to hinder enzymatic hydrolysis. These constraints highlight the need for improved process configurations to enhance ozone

effectiveness and biomass accessibility [14–16]. These limitations highlight a critical research gap in improving the effectiveness of ozonolysis for lignocellulosic biomass conversion. In particular, the potential of process intensification through double-stage ozonolysis (D-Oz) has not been systematically explored. This double-stage approach is hypothesized to facilitate deeper structural disruption of biomass, leading to greater exposure of cellulose fibers and significantly improved enzymatic saccharification [12,17,18].

Furthermore, this research contributes to a deeper understanding of optimizing enzymatic saccharification parameters through the application of statistical tools such as Response Surface Methodology (RSM). The integration of advanced statistical modelling enables the identification of optimal conditions that maximize TRS production, while the use of ANOVA and regression analysis ensures methodological rigor and reliability of the experimental findings. This approach improves process efficiency by identifying the most influential variables affecting saccharification performance. In addition, kinetic results show that pretreatment significantly influenced the enzymatic saccharification of D-Oz OPEFB. Pretreatment lowered the  $K_m$  value, signifying improved enzyme binding and cellulose accessibility. The results suggest that D-Oz enhanced enzyme–substrate affinity and increased the saccharification potential of OPEFB for TRS production.

The objectives of this study were to propose a novel double-stage ozonolysis pretreatment, integrated with intermediate alkaline swelling, enhance ozone penetration, promote deeper lignin degradation, improve cellulose accessibility and ultimately increase total reducing sugar (TRS) yield. In addition, the enzymatic saccharification process was optimized using RSM-FCCD to identify the significant process variables affecting TRS production. The double-ozonolysis pretreatment strategy was designed to progressively disrupt the lignin–carbohydrate complex through sequential ozone oxidation and alkaline swelling, thereby enhancing cellulose exposure and enzyme accessibility. The kinetic behavior of enzymatic saccharification was subsequently evaluated using the Michaelis–Menten model and Lineweaver–Burk plot to determine  $K_m$  and  $V_{max}$ , which represent enzyme–substrate affinity and maximum catalytic rate, respectively. Together, optimization and kinetic analyses provide a comprehensive assessment of the double-ozonolysis pretreatment to enhance TRS production from OPEFB.

## 2. Materials and Methods

### 2.1. Chemicals

The chemicals, such as deionized water, sulphuric acid ( $H_2SO_4$ ), acetic acid ( $C_2H_4O_2$ ), nitric acid ( $HNO_3$ ), 3,5-dinitrosalicylic acid ( $C_7H_4N_2O_7$ ), sodium hydroxide (NaOH), sodium potassium tartarate ( $KNaC_4H_4O_6 \cdot 4H_2O$ ), commercial enzyme cellulase mixture, oxygen gas ( $O_2$ ), acetone ( $C_3H_6O$ ), sodium acetate trihydrate ( $CH_3COONa \cdot 3H_2O$ ), glacial acetic acid ( $C_2H_4O_2$ ) and sodium chlorite ( $NaClO_2$ ) was purchased as tabulated in Table 1.

### 2.2. Sample OPEFB Preparation

The OPEFB used in this study was obtained from Sedenak Palm Oil Mill. Upon collection, the raw OPEFB samples were dried, ground and sieved for 0.3mm particle size. Finally, the prepared OPEFB samples were stored in sealed containers at room temperature to prevent moisture reabsorption and contamination from the surrounding environment. This storage condition helps preserve the integrity of the biomass prior to further experimental use.

### 2.3. Hybrid Pretreatment of OPEFB

A total of 3 methods were employed for hybrid pretreatment of OPEFB including physical, ozonolysis and alkaline pretreatment.

#### 2.3.1. Physical pretreatment

The raw OPEFB was dried in direct sunlight for 8 h per day for a week and then heated up to 100 °C to remove inherent moisture, which is essential to prevent microbial degradation and to ensure consistent physicochemical properties during subsequent processing. Following drying,

the OPEFB was mechanically ground using the grinder (cutting mill SM-100, Germany) to reduce the fibre size. Then, the ground OPEFB was sieved using the mechanical sieve shaker (Biobase BK-TS200, China) with the mesh of 1.0 mm, 0.8 mm, 0.5 mm, 0.3 mm and 0.25 mm to obtain the desired particle size which was 0.3 mm.

#### 2.3.2. Ozonolysis pretreatment

##### 2.3.2.1. Single stage ozone pretreatment

Ozonolysis pretreatment of OPEFB was carried out by using the OzBiONY® 2.0 reactor located at N32, High Temperature Laboratory, Faculty of Chemical and Energy Engineering, Universiti Teknologi Malaysia. 500 g of OPEFB with particle size of 0.3 mm was charged into the horizontal reactor. The OPEFB sample was sprayed with water until the moisture content measured by using moisture analyser (MOC63u UNITBLOC) to be about 20 wt%. The ozone generator was set for 60 g/m<sup>3</sup> ozone concentration. The ozone was then supplied into the reactor for 90 min.

##### 2.3.2.2. Double-stage ozone pretreatment

After single-stage ozone pretreated sample was prepared, alkaline swelling was carried out using 5 % sodium hydroxide (NaOH) with a ratio of 1:10 % w/v at ambient temperature, 200 rpm for 1 h under vigorous stirring using mechanical stirrer. This alkaline swelling was required to further enhance the swelling of the crystalline cellulose structure, in addition to improve the removal of lignin and hemicellulose, thereby leading to an increase in the substrate surface area for enzymatic saccharification [17–19]. After 1 h, the sample was neutralised by adding acetic acid until it reached pH of 6-8. The sample was

Table 1. List of chemicals used in the experiment.

No.	Name of Chemicals	Purity (%)	Purchased from / Supplied by Brand
1	Deionised water	≥ 98	Vchem
2	Sulphuric acid ( $H_2SO_4$ )	98	Qrec
3	Acetic acid ( $C_2H_4O_2$ )	-	Sigma Aldrich
4	Nitric acid ( $HNO_3$ )	-	Merck
5	3,5-Dinitrosalicylic acid ( $C_7H_4N_2O_7$ )	99	Sigma Aldrich
6	Sodium hydroxide (NaOH)	≥ 99	Merck
7	Sodium potassium tartarate ( $KNaC_4H_4O_6 \cdot 4H_2O$ )	≥ 99	Millipore
8	Commercial Enzyme Cellulase Mixture	≥ 1000	Aladdin
9	Oxygen gas ( $O_2$ )	-	Mega Mount Industrial Gases
10	Acetone ( $C_3H_6O$ )	≥ 99.8	Merck
11	Sodium acetate trihydrate ( $CH_3COONa \cdot 3H_2O$ )	≥ 99	Fisher Scientific
12	Glacial acetic acid ( $C_2H_4O_2$ )	-	ACI Labscan
13	Sodium chlorite ( $NaClO_2$ )	80	Acros Organics

left overnight to make sure all bases were diluted, sample was tested using a pH meter to ensure the pH was neutral. Neutralised sample was filtered, washed and dried in an oven at 70 °C until a constant weight was achieved. Sample was kept inside the sealed bag for double ozone pretreatment. Prior to the second ozonolysis treatment, the same step as a single-stage ozone pretreated sample, the moisture content of the wet sample was determined to be 20 wt%. The ozone generator was set for 60 g/m<sup>3</sup> ozone concentration. The ozone was then supplied to the reactor for 180 minutes.

### 2.3.3. Alkaline pretreatment

Untreated OPEFB with particle size of 0.3 mm was prepared in a 200 g quantity. The untreated OPEFB was treated with 3% sodium hydroxide (NaOH) with a ratio of 1:10 % w/v at 110 °C, for 45 minutes and then bleached with 5 % w/v sodium chlorite (NaClO<sub>2</sub>) at 80 °C, for 60 minutes. At the end of reaction, the slurry was filtered using filter cloth. The slurry was neutralized by adding a drop by drop of acetic acid and washed using deionised water using mechanical stirrer until the pH range (6-8) is achieved. Tested with litmus paper and pH meter. The slurry was poured into a tray and dried in an oven at 60 °C for 24 h. The sample was kept inside desiccator with sealed bag.

### 2.3.4. Ozone-alkaline pretreatment

200 g sample from single-stage ozone pretreatment was taken for the next alkaline pretreatment to produce ozone-alkaline pretreated sample. The pretreatment conditions were 100 °C, 10 % sodium hydroxide (NaOH) with a ratio of 1:10 % w/v with 200 g of single-ozone pretreated samples. The samples were heated on a hotplate at constant stirring rate and covered with aluminium foil on top to avoid any contamination from the air. The reaction time was 3 h. After the reaction ended, the slurry was neutralized by adding acetic acid until it reached pH of 6-8. Sample was left overnight to make sure all bases were diluted and the sample was tested using a pH meter to ensure the pH was neutral. Neutralized sample was filtered, washed and dried in an oven at 60 °C until a constant weight was achieved. Sample was kept inside the sealed bag for analysis.

### 2.4. Chemical Composition Analysis of OPEFB

The untreated and pretreated OPEFB were analysed for cellulose, hemicellulose and lignin contents. The cellulose and hemicellulose contents of OPEFB were measured using the method described by Tan & Lee [20]. The lignin fractionated into acid-insoluble lignin (AIL) and

acid-soluble lignin (ASL), which were determined according to NREL laboratory analytical procedures as described by Rizal [22].

### 2.5. Thermal Analysis of OPEFB

Thermal Gravimetric Analyzer (Perkin Elmer TGA 4000) was used for thermal analysis of samples of untreated (raw), alkaline-treated (A-P), single-stage ozone pretreated (S-Oz), ozone-alkaline treated (Oz-Ap), double-stage ozone pretreated (D-Oz) OPEFB and commercial alpha-cellulose ( $\alpha$ -cell). Approximately 2 mg of the sample was heated in a platinum cell from 30 °C to 900 °C at a heating rate of 10 °C/min under a nitrogen atmosphere.

### 2.6. Determination of Crystallinity Index of OPEFB

X-ray diffraction (XRD) was employed for structural characterisation. The crystallinity and amorphousity of raw, A-P, S-Oz, Oz-Ap, D-Oz and  $\alpha$ -cell samples were evaluated using XRD analysis. The dried samples were scanned in 2 $\theta$  range from 10° to 50° using Cu radiation generated at 40 kV and 30 mA. The crystallinity index (CrI) of the samples was calculated according to the XRD peak height method [23], shown in Equation (1):

$$\text{CrI (\%)} = \frac{I_{\text{crystalline}} - I_{\text{amorphous}}}{I_{\text{crystalline}}} \times 100\% \quad (1)$$

### 2.7. Morphological Characteristics of OPEFB

Scanning electron microscopy (SEM) image was taken for raw, A-P, S-Oz, Oz-Ap, D-Oz and  $\alpha$ -cell samples. Dried samples were observed under SEM-Hitachi. SEM images of samples were recorded at 300 magnification using an accelerating voltage of 15 kV and work distance (WD) of 6.80 mm.

### 2.8. Functional Groups Observation of OPEFB

Fourier Transform Infra-Red (FTIR) analysis (Frontier Perkin Elmer) was used to characterize the functional groups of raw, A-P, S-Oz, Oz-Ap, D-Oz and  $\alpha$ -cell samples. IR spectra were recorded in an absorption mode with a scan count of 8 per sample and a resolution of 8 cm<sup>-1</sup> in the wave number range of 4000 and 400 cm<sup>-1</sup> at room temperature.

### 2.9. Optimization of Enzymatic Saccharification using Design Expert® Software

#### 2.9.1. Screening parameter of enzymatic saccharification

A screening parameter was conducted to evaluate the effects of several operational parameters on the performance of enzymatic

saccharification. The screening was performed using the One-Factor-at-a-Time (OFAT) approach, where one independent variable was varied while the remaining parameters were kept constant. Based on commonly reported parameters in previous literature, three key factors were selected for this study. This includes reaction time (4-44 h), D-Oz biomass loading (0.2-5.0 % w/v) and temperature (25-60 °C). The significant factors identified through OFAT were subsequently selected for further optimization.

### 2.9.2. Response Surface Methodology for optimization

Response Surface Methodology (RSM) is a statistical technique that is widely used to evaluate the interaction between several independent variables to determine the optimal operating conditions of significant process parameters. In this study, RSM was employed to optimize the enzymatic saccharification for TRS production. A three-level face-centered central composite design (FCCCD) with an axial distance of  $\alpha = 1$  was applied using Design-Expert software (v.13). The FCCCD was selected due to its effectiveness in modeling quadratic response and reducing the number of experimental trials while maintaining statistical reliability [24,25].

Based on the results obtained from the preliminary OFAT screening, the range of three independent variables were adjusted for optimization which are reaction time (*A*), biomass loadings (*B*), and temperature (*C*). Each variable was studied at three levels, coded as -1 (low), 0 (center) and +1 (high). The range and coded levels of the experimental variables used in this study are presented in Table 2. Constant parameters throughout this experiment were an incubator speed of 200 rpm, an enzyme activity of 70 U/g, and a sodium acetate buffer at pH of 4.8.

### 2.10. Analysis of Total Reducing Sugar (TRS) via dinitrosalicylic acid (DNS) Method

The amount of TRS in the hydrolysate of enzymatic saccharification was determined by dinitrosalicylic acid (DNS) method. About 1 mL of each hydrolysate sample was mixed with 1 mL of DNS reagent, measured with a micropipette. The

mixtures were placed in 90 °C water bath for 5 minutes. The mixture was immediately cooled to room temperature before the UV-Vis spectroscopy analysis at 540 nm. Before the measurement, the hydrolysate sample was diluted at a certain dilution factor to obtain measurements within the accuracy of the UV-Vis spectrophotometer. The DNS reagent and buffer mixture was prepared as the blank sample. Blank solution was poured into a cuvette, and the absorbance was set to 0. The absorbance of other samples was then measured and recorded. The TRS concentration (mg/mL) in the hydrolysate of each sample was determined from the equation obtained from glucose standard calibration.

### 2.11. Evaluation of Enzymatic Behaviour towards Ozone-Pretreated during Enzymatic Saccharification

The evaluation of enzymatic behaviour towards ozone-pretreated OPEFB was conducted by using optimized conditions from DOE of enzymatic saccharification, by varying substrate loading and analyzing the TRS production. The enzymatic saccharification experiment was conducted using raw, A-P, S-Oz, Oz-Ap, D-Oz and  $\alpha$ -cell samples. The hydrolysate was analysed using DNS method to determine TRS content. Experimental runs were conducted in triplicate. Figure 1 shows Lineweaver-Burk plot of  $1/V$  versus  $1/[S]$ , where  $V$  is reaction rate,  $S$  is substrate concentration,  $K_m$  is the Michaelis-Menten constant,  $V_{max}$  is the maximum enzyme velocity of saccharification and  $V_o$  is enzyme velocity defined using Equation (2):

$$\frac{1}{v_0} = \frac{K_m}{V_{max}} \left[ \frac{1}{[S]} \right] + \frac{1}{V_{max}} \quad (2)$$

Following the derivation of linear equation of Equation 2), the maximum enzyme velocity ( $V_{max}$ )(mg/mL.min) and the Michaelis-Menten constant ( $K_m$ ) (mg/mL) were calculated using Equations (3) and (4):

Table 2. The factor levels for Face-Centered Central Composite Design (FCCCD).

Factors	Units	Levels of factors		
		-1	0	1
A: Reaction time	(h)	14	29	44
B: Biomass loading	(% w/v)	1.8	3.0	4.2
C: Temperature	(°C)	20	35	50

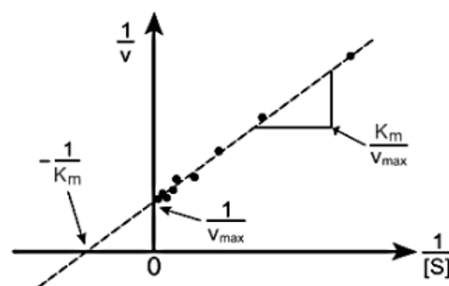


Figure 1. Lineweaver- Burk plot of  $1/V$  versus  $1/[S]$ .

$$V_{max} = \frac{1}{y\text{-intercept}} \quad (3)$$

$$K_m = V_{max} \cdot (\text{gradient of linear graph}) \quad (4)$$

### 3. Results and Discussions

#### 3.1. Physical Observation

Physical observation of all untreated and pretreated OPEFB based on Figure 2, untreated OPEFB raw exhibited a rigid, compact, and dark brown fibrous structure, which is typical of lignocellulosic biomass due to its high lignin content. This dense structure limits enzyme access to cellulose and reduces hydrolysis efficiency [26]. After alkaline pretreatment, A-P fibres became lighter, more swollen, and less compact, indicating partial lignin removal and increased porosity [27]. S-Oz appeared more fragmented and less rigid, showing that ozonolysis weakened the lignocellulosic structure through lignin degradation. Greater disruption was observed in the Oz-Ap, which showed a more fibrillated and porous structure due to the combined effect of ozone oxidation and alkaline solubilisation of lignin fragments. Among all samples, the sample D-Oz showed the most obvious change, with lighter and more separated fibres, closely resembling commercial  $\alpha$ -cellulose. This suggests extensive removal of non-cellulosic components and enrichment of cellulose. Overall, the physical changes observed after pretreatment confirm the effective removal of lignin and

hemicellulose, which improved the accessibility of cellulose for enzymatic saccharification and TRS production [3,16].

#### 3.2. Chemical Composition of Untreated and Treated OPEFB

Table 3 shows, raw OPEFB consisted of 39 wt% cellulose, 33.4 wt% hemicellulose, and 22 wt% AIL, reflecting the typical recalcitrant lignocellulosic structure. Following pretreatment, substantial compositional changes were observed, particularly in lignin removal and cellulose enrichment. Among all pretreatment strategies, D-Oz resulted in the highest cellulose content (79 wt%), approaching that of commercial  $\alpha$ -cellulose (~80 wt%), and significantly outperforming both single ozonolysis (S-Oz, 61 wt%) and the ozone-alkaline sequence (Oz-Ap, 66 wt%). This pronounced improvement can be attributed to the enhanced effectiveness of sequential oxidative degradation mechanisms in the double ozonolysis process.

The superior performance of D-Oz is primarily due to repeated ozone exposure, which enables progressive and deeper lignin depolymerization. During the first ozonation stage, ozone preferentially attacks electron-rich aromatic rings and unsaturated bonds in lignin, leading to partial delignification and disruption of the LCC. However, residual lignin particularly condensed and less reactive structures, remains

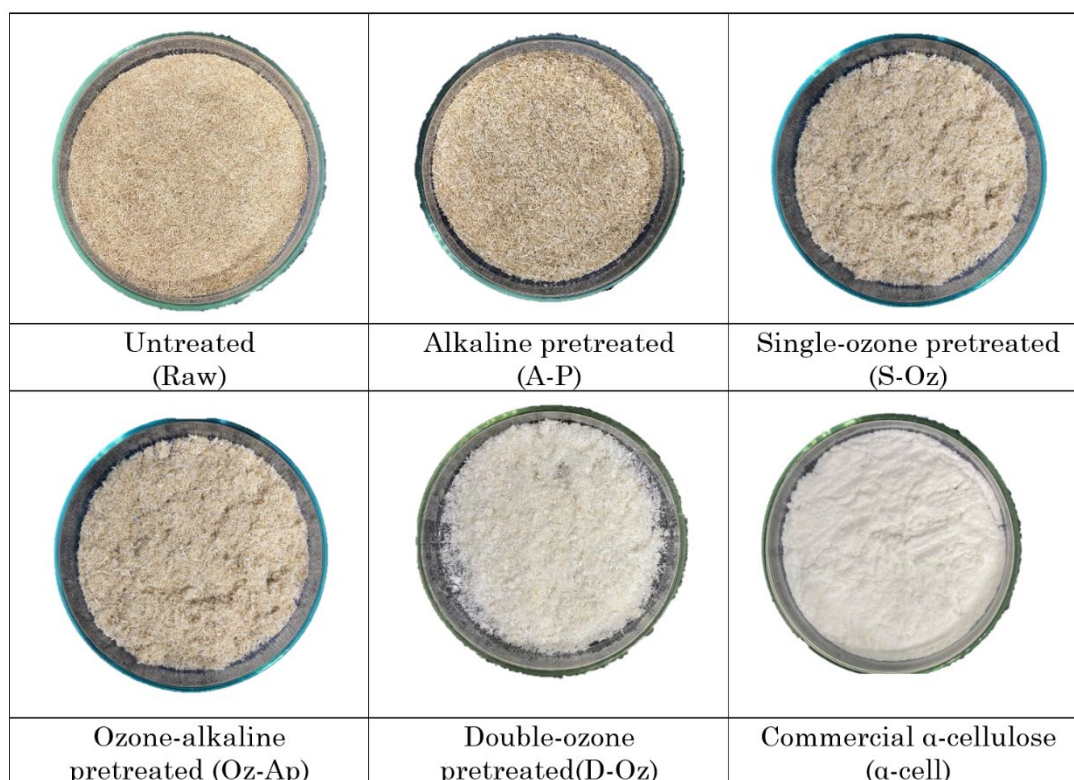


Figure 2. Physical observation of raw, A-P, S-Oz, Oz-Ap, D-Oz,  $\alpha$ -cell samples.

embedded within the biomass matrix. The second ozonation stage further oxidizes these recalcitrant lignin fractions, resulting in more complete lignin removal and greater exposure of cellulose fibers. Recent studies [18,19,30] have shown that oxidative pretreatment significantly enhances lignin degradation due to improved accessibility and cumulative oxidative effects, leading to higher cellulose purity and enzymatic digestibility.

In contrast, the (Oz-Ap) sequence exhibited lower cellulose enrichment (66 wt%) compared to D-Oz. Although alkaline treatment promotes biomass swelling, lignin solubilization, and partial hemicellulose removal, it can also lead to lignin reprecipitation or condensation reactions, which reduce the effectiveness of subsequent ozone attack. Furthermore, alkaline pretreatment may alter lignin structure into more condensed forms that are less reactive toward ozone oxidation. As a result, the second-stage ozone in the Oz-Ap sequence is less efficient in degrading residual lignin compared to a direct second ozonation stage.

Additionally, the double ozonolysis approach minimizes chemical interference and maintains a highly oxidative environment, allowing ozone to continuously target lignin without competing side reactions. This leads to more selective lignin removal, lower hemicellulose content (9.5 wt%), and higher cellulose enrichment, as observed in Table 3. The progressive breakdown of lignin in D-Oz also improves pore structure and internal

surface area, facilitating better mass transfer and accessibility for subsequent enzymatic hydrolysis.

Overall, the results demonstrate that double-stage ozonolysis is more effective than both single ozonolysis and ozone-alkaline pretreatment due to its ability to overcome mass transfer limitations, achieve deeper lignin degradation, and avoid lignin condensation effects. This explains the significant compositional changes observed and highlights the advantage of D-Oz in producing highly enriched cellulose suitable for efficient saccharification.

### 3.3. Thermal Analysis of OPEFB

The thermal degradation behaviour of untreated and pretreated OPEFB samples was evaluated using TGA analysis, while the corresponding degradation rates were analyzed using derivative thermogravimetric (DTG) curves, as shown in Figure 3(a) and Figure 3(b). These analyses provide valuable insights into the thermal stability and structural composition of the biomass following different pretreatment methods. Three distinct stages of degradation were observed. The first stage, occurring below 100 °C, involved minor weight loss attributed to moisture evaporation. The second stage corresponded to the main decomposition region, where significant degradation occurred between 200 and 350 °C. In this region, hemicellulose and lignin primarily decomposed at 250–300 °C, while

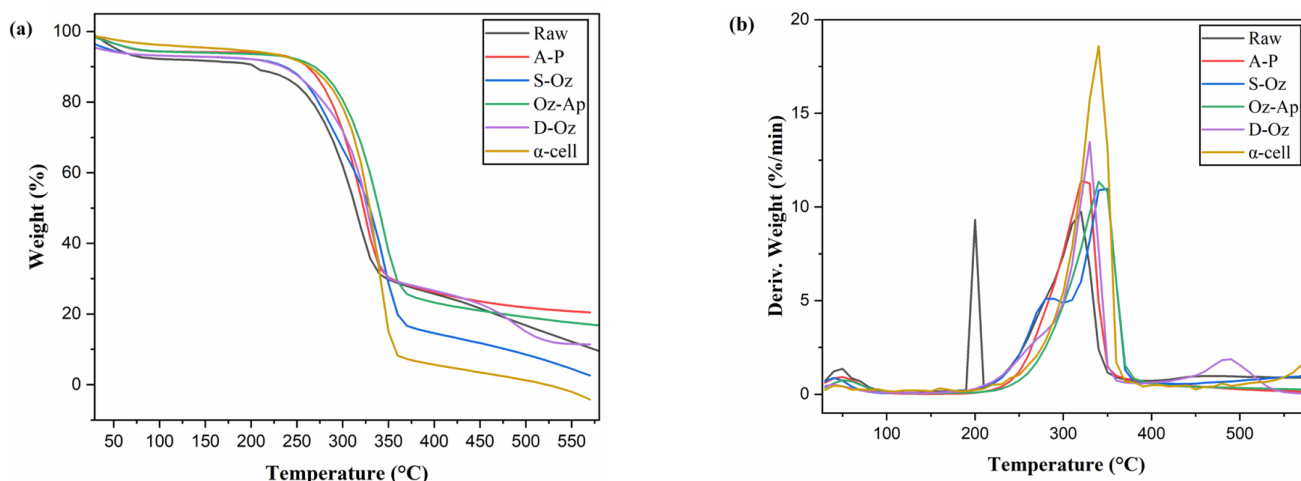


Figure 3. TGA curves (a) and DTG (b) curves for raw, A-P, S-Oz, Oz-Ap, D-Oz, α-cell.

Table 3. Chemical composition of untreated and pretreated OPEFB.

Sample / Composition (wt%)	Raw	A-P	S-Oz	Oz-Ap	D-Oz	α-cell
Cellulose	39.00	50.00	61.00	66.00	79.00	~80.00
Hemicellulose	33.40	24.00	16.40	10.60	9.50	NA
Acid Insoluble Lignin (AIL)	22.00	3.38	1.67	3.00	2.34	NA
Acid Soluble Lignin (ASL)	0.27	0.07	0.07	0.05	0.07	NA
Others	5.33	22.55	20.87	20.35	7.87	NA

cellulose degradation occurred at a higher temperature range of 380–400 °C. The raw sample exhibited earlier weight loss, indicating lower thermal stability due to the presence of hemicellulose and amorphous lignin. In contrast, pretreated samples exhibited delayed degradation at higher temperatures, indicating partial removal of hemicellulose and lignin, along with the enrichment of cellulose. Among the pretreated samples, Oz-Ap and D-Oz demonstrated slower weight loss and higher decomposition temperatures, indicating more effective pretreatment. The DTG curves further supported these findings, with the raw sample exhibiting a lower maximum degradation temperature ( $T_{max}$ ), while A-P and S-Oz shifted to slightly higher values. Notably, D-Oz and Oz-Ap exhibited sharper DTG peaks, approaching that of  $\alpha$ -cellulose, indicating higher cellulose purity. Therefore, the thermal analysis confirms that pretreatment significantly alters the thermal behaviour of OPEFB by reducing lignin and hemicellulose content, increasing cellulose enrichment, and enhancing its suitability for enzymatic saccharification and TRS production [28].

### 3.4. Determination of Crystallinity Index of OPEFB

The crystalline structure of cellulose in lignocellulosic biomass was characterized using XRD to assess structural changes induced by pretreatment. Cellulose comprises both crystalline and amorphous regions, where the crystalline regions consist of highly ordered cellulose chains stabilized by extensive hydrogen bonding, while the amorphous regions are less ordered and more accessible to chemical and enzymatic attack [29]. The crystallinity index (CrI) is used to estimate the relative proportion of crystalline cellulose and to evaluate structural

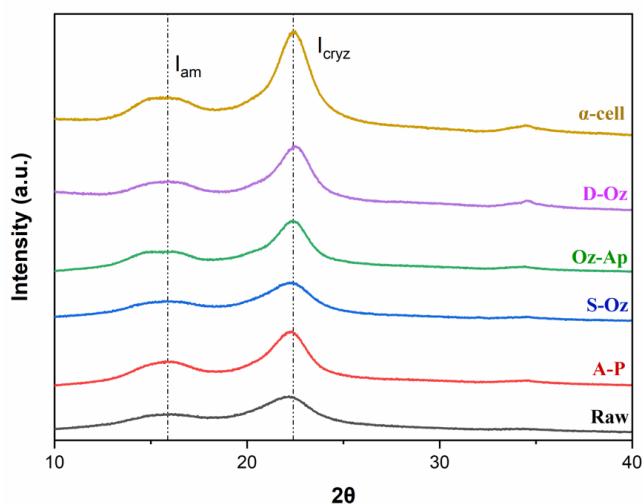


Figure 4. XRD plots of raw, A-P, S-Oz, Oz-Ap, D-Oz and  $\alpha$ -cell.

modifications following pretreatment, as presented in Figure 4 and Table 4. In this study, raw OPEFB exhibited CrI of 47.42%, indicating a moderate degree of crystallinity within the lignocellulosic matrix. Following pretreatment, the crystallinity varied depending on the method employed. For instance, single-ozone pretreatment reduced the CrI to 40.19%, possibly attributed to partial disruption of the cellulose structure and alteration of its ordered arrangement. In contrast, double-ozone pretreatment significantly increased the CrI to 72.18%, a value comparable to that of commercial  $\alpha$ -cellulose (72.46%). This increase is primarily associated with the removal of amorphous components, such as lignin and hemicellulose, resulting in a higher relative fraction of crystalline cellulose [23]. However, an increase in crystallinity does not necessarily correspond to reduced enzymatic hydrolysis efficiency. Instead, it often reflects the effective elimination of non-crystalline fractions and the enhanced exposure of cellulose microfibrils. Consequently, enzyme accessibility can be improved despite the higher crystalline content [30]. Accordingly, crystallinity analysis provides critical insight into the structural modifications of OPEFB induced by pretreatment, particularly regarding biomass digestibility and subsequent conversion efficiency.

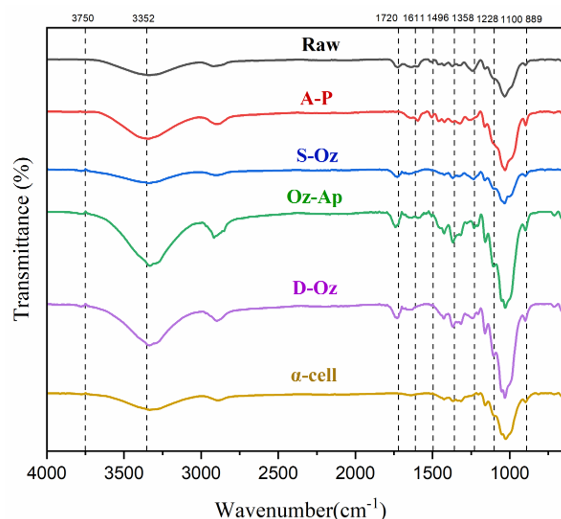


Figure 5. FTIR spectra for raw, A-P, S-Oz, Oz-Ap, D-Oz and  $\alpha$ -cell.

Table 4. Crystallinity index for untreated and pretreated OPEFB.

Type of sample	CrI(%)
Raw	47.42
A-P	47.13
S-Oz	40.19
Oz-Ap	49.44
D-Oz	72.18
$\alpha$ -cell	72.46

### 3.5. Functional Groups Observation of OPEFB

FTIR spectroscopy was employed to characterize structural changes in raw and pretreated OPEFB samples, as shown in Figure 5. The main absorption bands in Table 5 were identified at 3352–3750  $\text{cm}^{-1}$ , 1611–1720  $\text{cm}^{-1}$ , 1358  $\text{cm}^{-1}$ , and 889–1496  $\text{cm}^{-1}$ , corresponding to hydroxyl groups, lignin, hemicellulose, and cellulose-related bonds, respectively. In the raw OPEFB sample, the distinct peaks observed at 1611–1720  $\text{cm}^{-1}$  and 1358  $\text{cm}^{-1}$  confirm the presence of lignin and hemicellulose, while the bands in the range of 889–1496  $\text{cm}^{-1}$  are characteristic of the cellulose structure [31]. Following pretreatment, a progressive reduction in the intensity of lignin and hemicellulose-associated bands was observed, indicating the effective removal of non-cellulosic components. This reduction was particularly pronounced in the ozonolysis-treated samples, especially in the double ozonolysis (D-Oz) sample, where these peaks were greatly diminished. Meanwhile, the cellulose-related bands remained strong, showing that the cellulose backbone was preserved. Notably, the FTIR spectrum of D-Oz was also similar to that of commercial  $\alpha$ -cellulose, indicating a substantial enrichment of cellulose content. Therefore, the FTIR results confirmed that pretreatment, particularly double ozonolysis, effectively removes lignin and hemicellulose while maintaining the structural integrity of cellulose. These structural modifications are crucial for enhancing enzyme accessibility and improving enzymatic saccharification efficiency and TRS production [32].

### 3.6. Morphological Characteristics of OPEFB

The raw OPEFB (Figure 6a) exhibited a compact, rigid, and highly ordered surface covered with silica bodies and a dense lignin layer. This intact structure acts as a physical barrier that limits enzyme accessibility to cellulose fibres [33]. After alkaline pretreatment (Figure 6b), the biomass surface became relatively smoother with the formation of visible pores. This change is attributed to the swelling effect of NaOH, which disrupts ester linkages in the lignin–carbohydrate complex and partially solubilizes lignin and hemicellulose. As a result, internal fibre structures are loosened, increasing porosity but still maintaining the overall fibre integrity. Recent studies [17,18] confirm that alkaline pretreatment primarily causes fibre swelling and partial delignification without extensive structural fragmentation.

In contrast, ozonolysis pretreatment (Figure 6c and 6d) produced more pronounced surface disruption. Ozone acts as a strong oxidizing agent that selectively attacks lignin aromatic rings and unsaturated bonds, leading to oxidative cleavage of lignin macromolecules. This results in surface erosion, rupture formation, and increased pore

Table 5. FTIR peak positions and respective functional groups for raw, A-P, S-Oz, Oz-Ap, D-Oz and  $\alpha$ -cell.

Wavenumber ( $\text{cm}^{-1}$ )	Functional Group
889-1496	C-O & C-O-C (cellulose & B-glycosidic bond)
1358	-CH <sub>2</sub> (hemicellulose)
1611-1720	C=O (lignin)
3352-3750	-OH

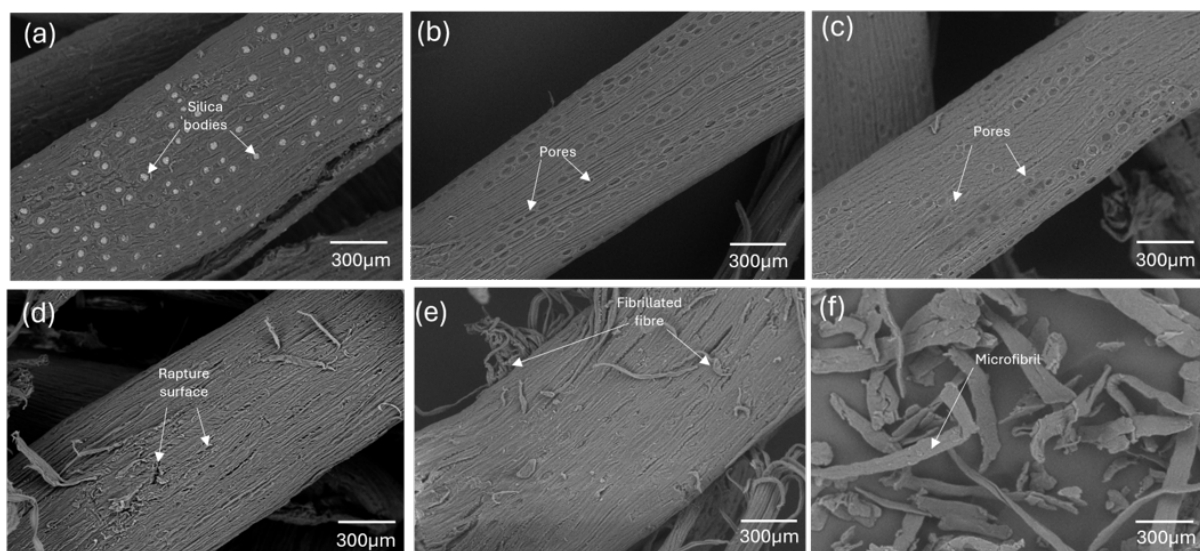


Figure 6. SEM images of (a) Raw (b) A-P (c) S-Oz (d) Oz-A (e) D-Oz (f)  $\alpha$ -cell at magnification 300 $\times$ .

development. Compared to alkaline treatment, ozonolysis generates a more heterogeneous and disrupted structure, as observed in the rupture surfaces (Figure 6d). However, in single ozonolysis, the disruption is still limited by ozone diffusion constraints and incomplete penetration into inner biomass layers, leaving some structural regions intact.

The most significant morphological transformation was observed in the double-stage ozonolysis sample (Figure 6e), where the biomass exhibited a highly fibrillated, fragmented, and open structure. This can be explained by the cumulative oxidative effect of repeated ozone exposure. The first ozonation partially removes lignin and opens up the structure, while the second ozonation penetrates deeper into the loosened matrix, leading to extensive delignification and fibre separation into microfibrils. This progressive degradation results in a structure that closely resembles commercial  $\alpha$ -cellulose (Figure 6f), characterized by well-separated microfibrils and minimal amorphous matrix.

Compared to the ozone-alkaline sequence, double ozonolysis provides a more uniform and extensive disruption because it avoids intermediate chemical modification that may cause lignin degradation and fibre separation [26]. Instead, continuous oxidative treatment maintains high reactivity toward lignin, resulting in greater structural breakdown, higher surface area, and improved pore connectivity. Overall, these morphological changes improved enzyme accessibility and supported higher TRS production.

### 3.7. Optimization of Enzymatic Saccharification using Design Expert® Software

#### 3.7.1. Parameter range selection of enzymatic saccharification

As summarized in Table 6 the parameters investigated included reaction time (4–44 h), biomass loading (0.2–5.0 % w/v), and temperature (25–60 °C). The screening results identified 24 h reaction time, 3.4 % w/v biomass loading, and 50 °C as the best preliminary conditions for enhanced TRS production.

Table 6. Best condition parameter screening of enzymatic saccharification.

Independent variables	Range	Best condition
Reaction time (h)	4-44	24
Biomass loading (% w/v)	0.2-5.0	3.4
Temperature (°C)	25-60	50

The OFAT method is an essential initial tool for establishing parameter ranges before optimization. Enzymatic hydrolysis efficiency depends on substrate accessibility, enzyme stability, and reaction kinetics. Pretreatment via double ozonolysis lowers lignin content, thereby increasing cellulose accessibility and cellulase susceptibility. However, saccharification remains sensitive to process variables like temperature and substrate concentration [34,35]. The OFAT parameter ranges provided a basis for later statistical optimization using response surface methodology (RSM).

#### 3.7.1.1 Effect of reaction time on enzymatic saccharification

Figure 7 shows that TRS concentration increased from 4 h to 24 h, then increased more slowly as the hydrolysis approached saturation. The rapid increase at the early stage was due to effective enzymatic hydrolysis of exposed cellulose after double ozone pretreatment, which improved fibre porosity and enzyme accessibility [36]. After 24 h, the reaction rate declined due to substrate depletion and possible glucose inhibition of cellulase activity [37].

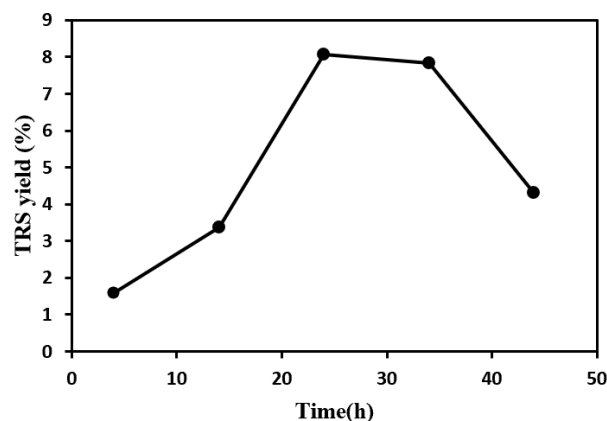


Figure 7. TRS yield versus time for double ozone pretreated OPEFB.

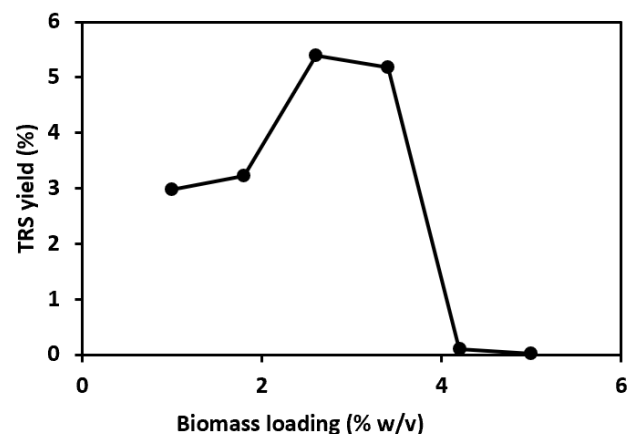


Figure 8. TRS yield versus biomass loading for double ozone pretreated OPEFB.

3.7.1.2 Effect of biomass loading on enzymatic saccharification

Figure 8 shows that TRS production increased with biomass loading up to 3.4 % w/v and then decreased at higher loadings. This is because moderate biomass loading improves enzyme–substrate interaction, while excessive loading increases slurry viscosity, reduces mixing, and limits enzyme access to the substrate [38]. Therefore, 3.4 % w/v was the optimum biomass loading for TRS production.

3.7.1.3 Effect of temperature on enzymatic saccharification

Figure 9 shows that TRS production increased from 25 °C to 50 °C and reached its maximum at 50 °C. This indicates that enzymatic saccharification was most effective at this temperature, which is within the optimum range for commercial cellulase activity (45–55 °C) [39]. Above 50 °C, enzyme denaturation may occur, reducing catalytic efficiency and TRS production.

3.8. Response Surface Methodology for Optimization

After OFAT screening, FCCCD under RSM optimized reaction time (A), biomass loading (B), and temperature (C), influencing TRS production as shown in Table 7. TRS yields varied, indicating complex interactions. The highest yield occurred at 44 h, 1.8 % w/v biomass, and 50 °C, demonstrating synergy between enzyme exposure and temperature. RSM effectively models quadratic and interaction effects, making it superior to OFAT for ES optimization.

3.9. Statistical Analysis

Table 8 shows that the quadratic model was significant (F-value = 7.53, p = 0.003), with temperature as the most significant factor, followed by biomass loading and reaction time.

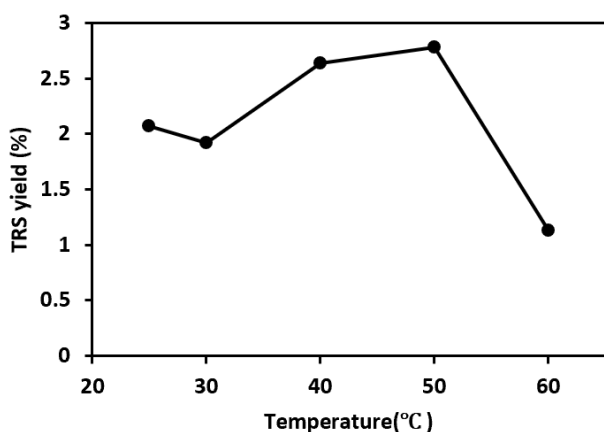


Figure 9. TRS yield versus temperature for double ozone pretreated OPEFB.

The non-significant lack-of-fit (p = 0.1193) indicated a good model fit [6]. In addition, the R<sup>2</sup> value of 0.8828 and adequate precision of 11.1846 confirmed that the model was reliable for predicting optimum TRS production conditions [40].

Mathematical prediction model expressed in Equation (5):

$$\begin{aligned} \text{Total Reducing Sugar Concentration} &= -11.7009 + 0.692098A + (-4.0568B) + \\ &1.71042C + (-0.147138AB) + (-0.008827AC) + \\ &(-0.097336BC) + 0.004551 A^2 + 1.34936 B^2 + \\ &(-0.011472C^2) \end{aligned} \quad (5)$$

3.10. Response Surface and Contour Plot Analysis

The contour and response surface plots in Figure 10 indicate that maximum TRS production was achieved at 44 h, 1.8% w/v biomass loading, and 50 °C. Figure 10(a) show the interaction between reaction time and biomass loading reveals that TRS production increased with prolonged reaction time, particularly at lower biomass loading. This trend is consistent with previous findings that extended hydrolysis time enhances enzyme–substrate interaction, leading to improved saccharification efficiency [41]. However, at higher biomass concentrations, TRS yield declined, likely due to increased slurry viscosity, which restricts enzyme accessibility to cellulose fibres.

Figure 10(b) illustrates the interaction between biomass loading and temperature, where the highest TRS production was observed at low biomass loading and elevated temperature. This suggests that although higher temperatures (~40–45 °C) enhance enzymatic activity and substrate solubility, excessive substrate concentration can hinder hydrolysis efficiency due to substrate inhibition and poor mixing conditions. Similar observations have been reported in recent studies on lignocellulosic biomass conversion, where optimal substrate loading is critical to avoid diffusion limitations and maintain effective enzyme performance [42].

In Figure 10(c), the interaction between reaction time and temperature demonstrates that TRS production increased significantly at longer reaction times and higher temperatures. Temperature exhibited a stronger individual effect on TRS yield, which aligns with ANOVA results [43]. This can be attributed to enhanced enzymatic kinetics and improved disruption of lignocellulosic structure at elevated temperatures, especially following oxidative pretreatment such as ozonolysis. Ozonolysis is known to selectively degrade lignin and increase cellulose accessibility, thereby amplifying the positive effect of temperature on enzymatic saccharification.

Table 7. The experimental results of Face-centred Central Composite Design (FCCCD).

Standard Run	Factor A	Factor B	Factor C	Response	
	A: Reaction time	B: Biomass loading	C: Temperature	Total Reducing Sugar Yield	
	(h)	(% w/v)	(°C)	Actual value	Predicted value
1	14	1.8	20	17.17	15.62
2	14	4.2	20	14.81	15.34
3	44	4.2	20	19.23	20.19
4	14	1.8	50	35.68	33.88
5	44	1.8	50	42.75	41.37
6	14	4.2	50	27.44	26.59
7	44	4.2	50	22.78	23.49
8	14	3.0	35	19.82	23.49
9	44	3.0	35	29.95	29.67
10	29	1.8	35	27.31	32.04
11	29	4.2	35	24.3	22.96
12	29	3.0	20	17.51	17.58
13	29	3.0	50	25.05	28.37
14	29	3.0	35	23.8	25.56
15	29	3.0	35	26.21	25.56
16	29	3.0	35	24.42	25.56
17	29	3.0	35	27.45	25.56
18	29	3.0	35	29.45	25.56
19	29	3.0	35	28.77	25.56

Table 8. ANOVA for the quadratic model of TRS yield.

Source	Sum of Squares	df	Mean Square	F-value	p-value	
Model	697.92	9	77.55	7.53	0.003	significant
A-Reaction time	64.17	1	64.17	6.23	0.034	
B-Biomass loading	138.93	1	138.93	13.5	0.0051	
C-Temperature	195.91	1	195.91	19.03	0.0018	
AB	34.98	1	34.98	3.4	0.0984	
AC	19.67	1	19.67	1.91	0.2002	
BC	15.31	1	15.31	1.49	0.2537	
A <sup>2</sup>	2.81	1	2.81	0.2726	0.6142	
B <sup>2</sup>	10.11	1	10.11	0.9817	0.3477	
C <sup>2</sup>	17.83	1	17.83	1.73	0.2207	
Residual	92.64	9	10.29			
Lack of Fit	66.4	4	16.60	3.16	0.1193	not significant
Pure Error	26.24	5	5.25			

Among the studied variables, biomass loading and temperature showed the strongest interaction, as indicated by the elliptical contour pattern. This interaction highlights the balance required between substrate availability and

process conditions to optimise hydrolysis efficiency. Overall, these findings confirm that TRS production is governed by the synergistic effects of process variables, where optimal temperature and controlled biomass loading are

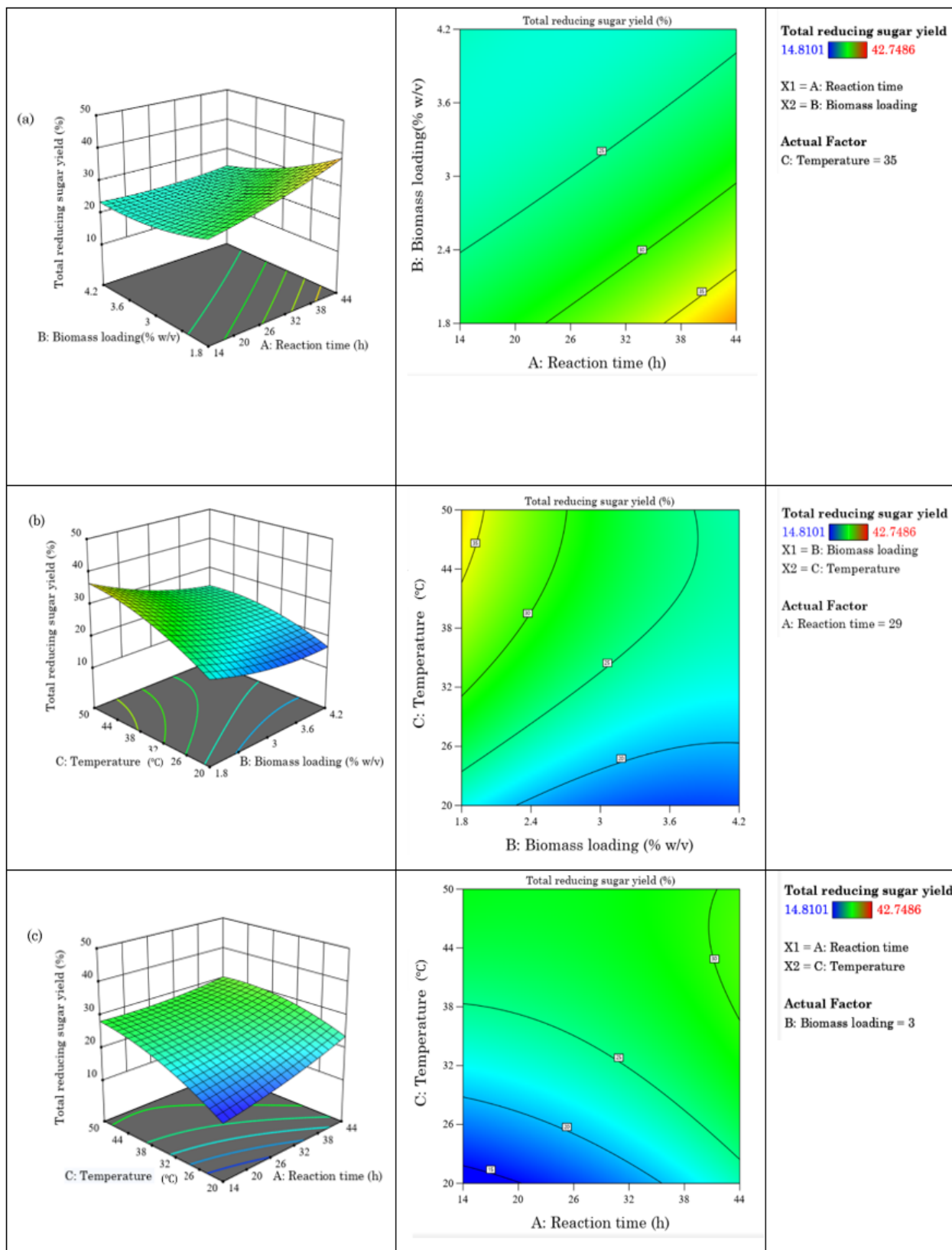


Figure 10. 3D Response Surfaces and contour plots of TRS production using fixed parameters at incubator speed of 200 rpm, an enzyme activity of 70 U/g, and a sodium acetate buffer of pH of 4.8.

essential for maximising enzymatic saccharification of double-stage ozone-pretreated OPEFB. These results are in agreement with recent optimisation studies emphasizing the importance of integrating physicochemical pretreatment with controlled hydrolysis parameters to achieve high sugar yields.

### 3.11. Experimental Validation of Optimized Conditions

The validation experiment was run at a randomised point, as shown in Table 9. A prediction error below 15% is generally considered acceptable and indicative of a reliable model with good predictive capability for process optimization.

### 3.12. Comparison with Untreated and Pretreated OPEFB

Experiments conducted under optimized conditions demonstrated clear differences in TRS yields among the various pretreatment strategies, as illustrated in Figure 11. The raw OPEFB exhibited a very low TRS yield (~3–4%), confirming the inherent recalcitrance of lignocellulosic biomass due to the rigid lignin-carbohydrate complex that limits enzyme accessibility. This observation is consistent with recent findings that highlight lignin as a major barrier to enzymatic saccharification due to non-productive enzyme adsorption and structural

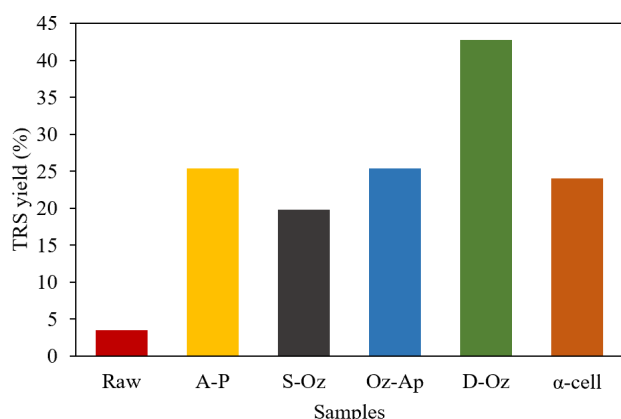


Figure 11. TRS yield under optimized conditions (44 h, 1.8% (w/v) biomass loading, and 50 °C) for raw, A-P, S-Oz, Oz-Ap, D-Oz and α-cell samples.

resistance [45].

Among the single-step pretreatments, alkaline-pretreated (A-P) and single ozonolysis (S-Oz) samples achieved moderate TRS yields (~25% and ~20%, respectively). The alkaline pretreatment likely enhanced enzymatic hydrolysis through partial lignin solubilization and hemicellulose removal, thereby increasing cellulose accessibility. However, its effectiveness is often limited by incomplete delignification and possible carbohydrate degradation. Similarly, single-step ozonolysis improved TRS yield via selective oxidative cleavage of lignin aromatic structures, but the extent of lignin disruption remained insufficient for maximum saccharification efficiency. Recent studies [18,19,30] have shown that oxidative pretreatment such as ozonation improve cellulose digestibility primarily by reducing lignin content and decreasing enzyme inhibition, although single-stage processes may not fully eliminate lignin recalcitrance.

A further increase in TRS yield was observed for the combined pretreatment (Oz-Ap), indicating a synergistic effect between ozonolysis and alkaline treatment. This improvement can be attributed to enhanced lignin fragmentation and increased porosity, which facilitates enzyme penetration and substrate accessibility. Similar synergistic pretreatment strategies have been reported to significantly enhance enzymatic hydrolysis efficiency by modifying lignin structure and reducing enzyme-binding inhibition.

Notably, the highest TRS yield (42.75%) was obtained from double ozonolysis (D-Oz), as shown in Figure 11, demonstrating its superior effectiveness compared to both single-step and combined pretreatments. The enhanced performance of D-Oz can be attributed to double oxidative delignification, which leads to more extensive lignin degradation, increased surface area, and improved cellulose exposure. Furthermore, ozone-induced structural modifications increase electrostatic repulsion between lignin and enzymes, further improving hydrolysis performance.

Interestingly, the TRS yield of D-Oz-treated OPEFB exceeded that of α-cellulose (~24%), suggesting that optimized pretreatment not only removes lignin but also induces favourable

Table 9. Validation experiment for optimization of TRS yield.

Parameter	Conditions		
Reaction Time(h)	44		
Biomass Loading (% w/v)	1.8		
Temperature (°C)	20		
Response	Predicted value (%)	Actual value (%)	% Error
TRS yield	31.06	26.41	14.98

structural changes such as reduced crystallinity and increased amorphous regions, which enhance enzyme accessibility. This observation aligns with recent reports indicating that effective oxidative pretreatment can outperform untreated or even purified cellulose in enzymatic hydrolysis due to improved substrate–enzyme interactions.

Overall, the results clearly demonstrate that while alkaline and single ozonolysis pretreatments improve saccharification efficiency, double ozonolysis provides a significantly enhanced effect. This confirms that extensive delignification achieved through double ozonolysis enhanced cellulose accessibility and enzymatic digestibility. Ozonolysis selectively degrades lignin aromatic structures without damaging cellulose backbone, thereby improving saccharification [46].

### 3.13. Kinetic Mechanism and Enhanced Enzymatic Behaviour of Ozone Pretreated OPEFB

The Lineweaver–Burk plots in Figure 12 (a-c) were used to determine kinetic parameters summarized in Table 10. The Michaelis–Menten kinetic analysis showed that ozonolysis pretreatment improved cellulase affinity toward OPEFB. The  $K_m$  value decreased markedly from 175.71 mg/mL for raw OPEFB to 32.38 mg/mL for single-ozone and 9.01 mg/mL for double ozone, indicating much stronger enzyme–substrate affinity after pretreatment [44,45]. This confirms that ozonolysis enhanced cellulose accessibility through lignin removal and increased exposed surface area. In contrast,  $V_{max}$  decreased from 0.005 mg/mL·min in raw OPEFB to 0.004

Table 10. Apparent kinetic parameters for raw, single-ozone and double-ozone pretreated OPEFB.

Parameter	D-Oz	S-Oz	Raw
Michaelis constant ( $K_m$ ) (mg/mL)	9.01	32.38	175.71
Limiting velocity ( $V_{max}$ )(mg/mL.min)	0.002	0.004	0.005

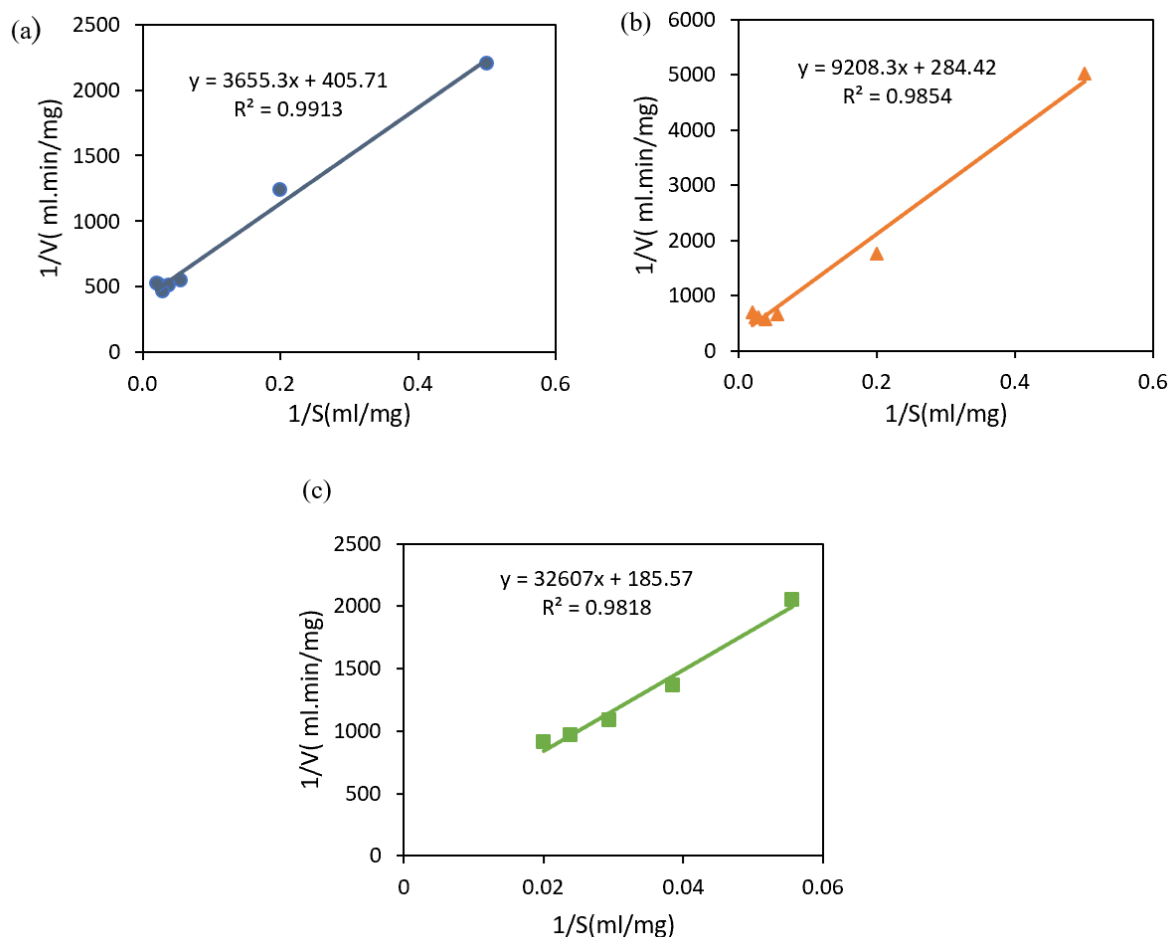


Figure 12. Lineweaver-Burk plot for (a) double-ozone pretreated OPEFB, (b) single-ozone pretreated OPEFB and (c) untreated OPEFB.

mg/mL·min in single-ozone and 0.002 mg/mL·min in double ozone, suggesting that structural modifications of the biomass influenced the maximum catalytic rate. Overall, the lower  $K_m$  values, especially for double ozone pretreatment, confirmed improved enzymatic saccharification efficiency for TRS production.

The schematic in Figure 13 illustrates the mechanisms of double-stage ozonolysis integrated with intermediate alkaline swelling followed by enzymatic saccharification for the valorization of OPEFB. Cellulose is a structural polysaccharide and a complex carbohydrate composed of long, linear chains of  $\beta$ -1,4-linked D-glucose units, typically ranging from several hundred to several thousand monomers. It serves as the primary structural component of plant cell walls, imparting rigidity and mechanical strength to plant tissues. The process begins with raw OPEFB, in which cellulose fibrils are embedded within a complex lignin–hemicellulose matrix that restricts enzyme accessibility. During the first ozonolysis stage, ozone ( $O_3$ ) selectively attacks the aromatic structures of lignin, leading to partial lignin depolymerization and disruption of the LCC. This is followed by alkaline swelling, which solubilizes residual lignin, removes part of the hemicellulose fraction, and induces fibre swelling, thereby increasing internal surface area and porosity. The subsequent second ozonolysis stage further enhances lignin degradation and promotes greater exposure of cellulose microfibrils, resulting in a more accessible and less recalcitrant structure. The enhanced

substrate is then subjected to enzymatic saccharification, involving a synergistic enzyme system consisting of exoglucanase (C) (specifically cellobiohydrolase),  $\beta$ -glucosidases (B), and endoglucanase (E). Endoglucanase targets amorphous regions of cellulose fibrils, attacking mid-chain bonds to break the cellulose into shorter cellodextrin chains. This step creates new reducing and nonreducing ends upon which cellobiohydrolase liberates some glucose units but primarily breaks cellulose down into cellobiose or longer oligosaccharides. Finally,  $\beta$ -glucosidase catalyzes end-chain hydrolysis of glycosidic bonds, extracting glucose from cellobiose and cellodextrin[46].

Overall, the combined pretreatment strategy significantly improves enzyme accessibility and catalytic efficiency, leading to enhanced conversion of lignocellulosic biomass into fermentable sugars, as enzyme adsorption and catalytic efficiency are strongly dependent on substrate surface area and porosity. This integrated mechanism highlights the effectiveness of process intensification in overcoming biomass recalcitrance and improving saccharification performance [23,47–49].

#### 4. Conclusion

This study demonstrated that double-stage ozonolysis pretreatment significantly enhanced the enzymatic saccharification of OPEFB by improving cellulose accessibility (up to 79 wt%) and reducing structural recalcitrance. Sequential ozonolysis effectively disrupts lignin through

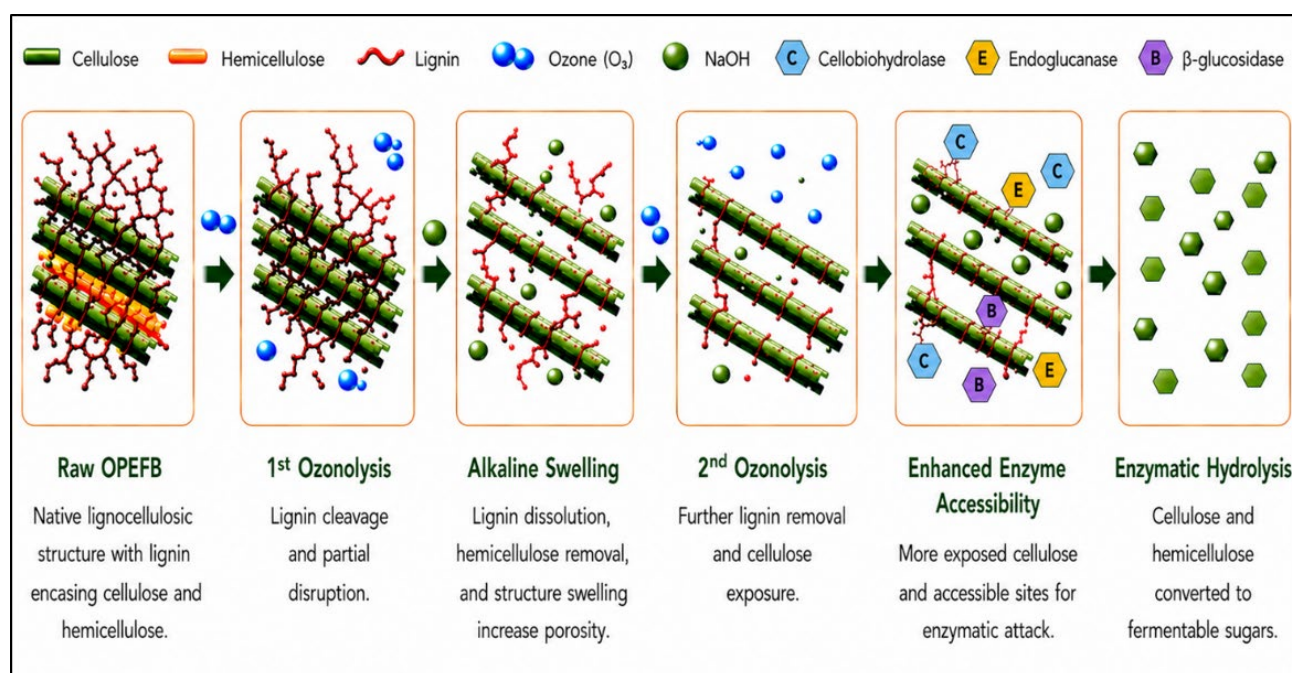


Figure 13. Schematic mechanisms of double-stage ozonolysis and alkaline swelling pretreatments of OPEFB, illustrating enhanced lignin removal, increased cellulose accessibility, and improved enzymatic conversion to fermentable sugars.

oxidative cleavage of aromatic structures, leading to increased porosity and exposure of cellulose fibres, thereby facilitating enzyme penetration and saccharification. Process optimisation using RSM identified optimal conditions of enzymatic saccharification of 44 h reaction time, 1.8% (w/v) biomass loading, and 50 °C achieving a maximum TRS yield of 42.75% with good model predictability ( $R^2 = 0.88$ ). Temperature was found to be the most influential factor affecting saccharification efficiency, followed by biomass loading and reaction time. Kinetic analysis revealed a substantial reduction in the Michaelis–Menten constant ( $K_m$ ) from 175.71 to 9.01 mg/mL, indicating enhanced enzyme–substrate affinity due to improved lignin removal and reduced non-productive enzyme binding. The double-stage ozonolysis approach provides more effective and uniform delignification compared to conventional methods, leading to improved hydrolysis performance. Overall, this study establishes double-stage ozonolysis as a robust and efficient pretreatment strategy for enhancing biomass-to-sugar conversion, with strong potential for sustainable biorefinery applications.

#### Acknowledgment

This work was supported by the Ministry of Education Malaysia under the Fundamental Research Grant Scheme (FRGS/1/2022/TK05/UTM/02/11), Embassy of France in Malaysia under France-Malaysia Collaboration Programme for Joint Research (MyTIGER) 2024 (Vot Number 1U072), Universiti Teknologi Malaysia Matching grant (Vot Number 05M00), and Malaysian Toray Science Foundation (MTSF) under Science and Technology Research Grant (Vot Number 4J754).

#### CRedit Author Statement

Author Contributions: Nur Zahidah Majid: Conceptualization, Methodology, Investigation, Resources, Data Curation, Writing, Review and Editing. Amnani Shamjuddin, Mohd Asmadi, Nur Hidayah Zainan, Nardiah Rizwana Jaafar, Umi Aisah Asli: Supervision, Conceptualization, Methodology, Formal Analysis, Data Curation. Asiah Nusaibah Masri: Validation, Data Curation. Riyani Tri Yulianti: Review and Editing. Gwendoline Christophe, Phillipe Michaud: Validation, Data Curation. All authors have read and agreed to the published version of the manuscript.

#### References

- [1] Bhattacharyya, S., Chakraborty, S., Dattaa, S., Drioli, E., Bhattacharjee, C. (2013). Production of total reducing sugar ( TRS ) from acid hydrolysed potato peels by sonication and its optimization. *Environmental Technology*, 34(9). DOI: 10.1080/09593330.2012.733965.
- [2] Mahardika, M., Zakiyah, A., Ulfa, S.M., Ahmad, R., Hassan, M.Z., Amelia, D., Knight, V.F., Nor, M. (2024). Recent Developments in Oil Palm Empty Fruit Bunch (OPEFB) Fiber Composite Recent Developments in Oil Palm Empty Fruit Bunch (OPEFB) Fiber. *Journal of Natural Fibers*, 21(1) DOI: 10.1080/15440478.2024.2309915.
- [3] Mankar, A.R., Pandey, A., Modak, A., Pant, K.K. (2021). Pretreatment of lignocellulosic biomass: A review on recent advances. *Bioresource Technology*, 334, 125235. DOI: 10.1016/j.biortech.2021.125235.
- [4] Malik, K., Sharma, P., Yang, Y., Zhang, P., Zhang, L., Xing, X., Yue, J., Song, Z., Nan, L., Yujun, S., El-Dalatony, M.M., Salama, E.S., Li, X. (2022). Lignocellulosic biomass for bioethanol: Insight into the advanced pretreatment and fermentation approaches. *Industrial Crops and Products*, 188, 115569. DOI: 10.1016/j.indcrop.2022.115569.
- [5] Harahap, B.M., Dewantoro, A.I., Maulid, M.R., Mardawati, E., Yarlina, V.P. (2020). Autoclave-assisted weak acid pretreatment of oil palm empty fruits bunches for fermentable sugar production. *IOP Conference Series: Earth and Environmental Science*, 443(1), 1–13. DOI: 10.1088/1755-1315/443/1/012080.
- [6] Woo, W.X., Tan, J.W., Tan, J.P., Indera Luthfi, A.A., Abdul, P.M., Abdul Manaf, S.F., Yeap, S.K. (2022). An Insight into Enzymatic Immobilization Techniques on the Saccharification of Lignocellulosic Biomass. *Industrial and Engineering Chemistry Research*, 61(30), 10603–10615. DOI: 10.1021/acs.iecr.2c01154.
- [7] Diyanilla, R., Hamidon, T.S., Suryanegara, L., Hussin, M.H. (2020). Overview of Pretreatment Methods Employed on Oil Palm Biomass in Producing Value-added Products : *BioResources*, 15(4), 9935–9997. DOI: 10.15376/biores.15.4.9935-9997.
- [8] Suhartini, S., Ainur, N., Hidayat, N., Idrus, S., Hoon, Y., Melville, L. (2023). Comparison of acid and alkaline pre-treatment on methane production from empty palm oil fruit bunches ( OPEFB ): Effect on characteristics , digester performance , and correlation of kinetic parameters. *Renewable Energy*, 215(July), 119009. DOI: 10.1016/j.renene.2023.119009.
- [9] Obeng, A.K., Premjet, D., Premjet, S. (2019). Combining Autoclaving with Mild Alkaline Solution as a Pretreatment Technique to Enhance Glucose Recovery from the Invasive Weed *Chloris barbata*. *Biomolecules*, 9(4), 120. DOI: 10.3390/biom9040120.

- [10]. Zhang, H., Han, L., Dong, H. (2021). An insight to pretreatment, enzyme adsorption and enzymatic hydrolysis of lignocellulosic biomass: Experimental and modeling studies. *Renewable and Sustainable Energy Reviews*, 140(12), 110758. DOI: 10.1016/j.rser.2021.110758.
- [11]. Orduña, J., Andrés, J., Vargas, M., Micali, O., Metzker, G., Gomes, E., Boscolo, M. (2019). Soaking and ozonolysis pretreatment of sugarcane straw for the production of fermentable sugars. *Industrial Crops & Products*, (May), 111959. DOI: 10.1016/j.indcrop.2019.111959.
- [12]. Shamjuddin, A., Ab Rasid, N.S., Michele Raissa, M.M., Abu Zarin, M.A., Wan Omar, W.N.N., Syahrom, A., Mohd Szali Januddi, M.A.F., Saidina Amin, N.A. (2021). Kinetic and dynamic analysis of ozonolysis pre-treatment of empty fruit bunch in a well-mixed reactor for sugar production. *Energy Conversion and Management*, 244(9), 114526. DOI: 10.1016/J.ENCONMAN.2021.114526.
- [13]. Ab Rasid, N.S., Shamjuddin, A., Abdul Rahman, A.Z., Amin, N.A.S. (2021). Recent advances in green pre-treatment methods of lignocellulosic biomass for enhanced biofuel production. *Journal of Cleaner Production*, 321, 129038. DOI: 10.1016/j.jclepro.2021.129038.
- [14]. Travaini, R., Martín-Juárez, J., Lorenzo-Hernando, A., Bolado-Rodríguez, S. (2015). Ozonolysis: An advantageous pretreatment for lignocellulosic biomass revisited. *Bioresource Technology*, 199, 2–12. DOI: 10.1016/J.BIORTECH.2015.08.143.
- [15]. Ethaib, S., Omar, R., Mustapa Kamal, S.M., Awang Biak, D.R., L. Zubaidi, S. (2020). Toward Sustainable Processes of Pretreatment Technologies of Lignocellulosic Biomass for Enzymatic Production of Biofuels and Chemicals: A Review. *BioResources*, 15(4), 10063–10088. DOI: 10.15376/biores.15.4.ethaib.
- [16]. Abdur Rasid, N.S., Shamjuddin, A., Saidina Amin, N.A. (2021). Chemical and structural changes of ozonated empty fruit bunch (EFB) in a ribbon-mixer reactor. *Bulletin of Chemical Reaction Engineering & Catalysis*, 16(2), 383–395. DOI: 10.9767/brec.16.2.10506.383-395.
- [17]. Arnandan, P.T., Wan Omar, W., Wan, N., Husna, Z., Sufri, M., Muhaimin, A., Akmal, D., Ahmad, J., Mba, M., Raissa, M., Shamjuddin, A., Chang, K., Aishah, N., Amin, S. (2025). Novel sequential ozonolysis-hydrolysis treatments for microcrystalline cellulose synthesis from oil palm empty fruit bunch. *Biomass and Bioenergy*, 199(January), 107902. DOI: 10.1016/j.biombioe.2025.107902.
- [18]. Mba Makam, R.M., Wan Omar, W.N.N., Thevi Arnandan, P., Abd Muhaimin, M.S., Jihat @ Ahmad, D.A., Shamjuddin, A., Hassan, Z.H., Chang, K., Saidina Amin, N.A. (2025). Sustainable carboxymethyl cellulose from ozonated empty fruit bunch for application as food coating additive. *International Journal of Biological Macromolecules*, 319(P4), 145660. DOI: 10.1016/j.ijbiomac.2025.145660.
- [19]. Mohd, N.H., Othaman, R., Mackeen, M.M., Maskat, M.Y. (2021). Effect of pretreatment and enzymatic hydrolysis for oligosaccharide production from oil palm mesocarp Fibre. *Sains Malaysiana*, 50(6), 1673–1683. DOI: 10.17576/jsm-2021-5006-14.
- [20]. Tan, H.T., Lee, K.T. (2012). Understanding the impact of ionic liquid pretreatment on biomass and enzymatic hydrolysis. *Chemical Engineering Journal*, 183, 448–458. DOI: 10.1016/j.cej.2011.12.086.
- [21]. Rizal, N.F.A.A., Ibrahim, M.F., Zakaria, M.R., Bahrin, E.K., Abd-Aziz, S., Hassan, M.A. (2018). Combination of superheated steam with laccase pretreatment together with size reduction to enhance enzymatic hydrolysis of oil palm biomass. *Molecules*, 23(4), 811. DOI: 10.3390/molecules23040811.
- [22]. Ahmad Rizal, N.F.A., Abd-aziz, S., Yee, P.L., Hassan, M.A. (2018). Pre-treatment of Oil Palm Biomass for Fermentable Sugars Production. *Molecules*, 23, 1–14. DOI: 10.3390/molecules23061381.
- [23]. Sari, F.P., Falah, F., Anita, S.H., Panji, K., Permana, R., Laksana, B., Fatriasari, W., Hermiati, E. (2021). Pretreatment of Oil Palm Empty Fruit Bunch ( OPEFB ) at Bench-Scale High Temperature-Pressure Steam Reactor for Enhancement of Enzymatic Saccharification. *Int Journal of Renewable Energy Development*, 10(2), 157–169. DOI: 10.14710/ijred.2021.32343.
- [24]. Yadav, V., Anand, A., Goyal, A. (2026). Enhanced enzymatic saccharification by statistically optimizing the delignification of bamboo biomass. *Biomass and Bioenergy*, 206(November 2025), 108646. DOI: 10.1016/j.biombioe.2025.108646.
- [25]. Brahma, D., Brahma, S., Kumar, Y. (2026). Face centered central composite design-Response surface methodology (FCC-RSM) a multivariate optimization of crystal violet dye adsorption by Cajanus cajan residues with thermodynamic, kinetic and mechanistic insights. *Next Materials*, 10(October 2025) DOI: 10.1016/j.nxmte.2025.101476.
- [26]. Hassan, Z.H., Saidina Amin, N.A., Wan Omar, W.N.N., Abd Muhaimin, M.S., Michele Raissa, M.M., Arnandan, P.T., Shamjuddin, A. (2026). Parametric Studies on Delignification using Ozonolysis Pretreatment of Oil Palm Empty Fruit Bunch for Cellulose Nano-fiber Production. *Journal of Advanced Research in Micro and Nano Engineering*, 42(1), 177–204. DOI: 10.37934/armne.42.1.177204.
- [27]. Seok, J., Lee, Y.Y., Hyun, T. (2016). Bioresource Technology A review on alkaline pretreatment technology for bioconversion of lignocellulosic biomass. *Bioresource Technology*, 199, 42–48. DOI: 10.1016/j.biortech.2015.08.085.
- [28]. Akindoyo, J.O., Ghazali, S.B., Beg, M.D.H. (2015). Structural and Thermal Properties of Ultrasound Treated Oil Palm Empty Fruit Bunch (Opefb) Fiber. *Tenth TheHER International Conference*, (February), 60–64.

- [29]. Mitbunrung, W., Rungraung, N., Muangpracha, N., Akanitkul, P., Winuprasith, T. (2022). Approaches for Extracting Nanofibrillated Cellulose from Oat Bran and Its Emulsion Capacity and Stability. *Polymers* 2022, Vol 14, Page 327, 14(2), 327. DOI: 10.3390/POLYM14020327.
- [30]. Liyana, N., Zailuddin, I. (2020). Morphology , mechanical properties , and biodegradability of all-cellulose composite films from oil palm empty fruit bunch. (July), 1–11. DOI: 10.1002/pls2.10008.
- [31]. Asmoro, N.W., Hidayat, C., Ariyanto, T., Millati, R. (2023). Cellulose Isolation From Oil Palm Empty Fruit Bunch Using Different Pretreatment Processes. *Journal of Applied Science and Engineering*, 26(11), 1513–1520. DOI: 10.6180/jase.202311\_26(11).0001.
- [32]. Hemashini, T., Lee, C.K., Goh, C.F., Tye, Y.Y., Ismayati, M., H'ng, Y.Y., Leh, C.P. (2024). Elucidating the Correlation of Lignocellulosic Compositions and Physicochemical Alterations in Oil Palm (*Elaeis guineensis*) Biomass on Enzymatic Saccharification Yield. *Bioenergy Research*, 17, 1612–1630. DOI: 10.1007/s12155-024-10762-3.
- [33]. Noor Arbaain, E.N., Kamal Bahrin, E., Ibrahim, M.F., Ando, Y., Abd-Aziz, S. (2019). Biological Pretreatment of Oil Palm Empty Fruit Bunch by *Schizophyllum commune* ENN1 without Washing and Nutrient Addition. *Processes*, 7(402), 2–8. DOI: 10.3390/pr7070402.
- [34]. Loh, S.K., Kassim, M.A., Bukhari, N.A. (2018). Optimisation of process conditions for ethanol production from enzymatically saccharified empty fruit bunch using response surface methodology (RSM). *Journal of Oil Palm Research*, 30(December), 642–654. DOI: 10.21894/jopr.2018.0045.
- [35]. Heris, S., Fitria, A., Nurfajrin, N., Fahriya, S., Sari, P., Risanto, L., Fatriasari, W. (2020). Optimization of Microwave-Assisted Oxalic Acid Pretreatment of Oil Palm Empty Fruit Bunch for Production of Fermentable Sugars. *Waste and Biomass Valorization*, 11(6), 2673–2687. DOI: 10.1007/s12649-018-00566-w.
- [36]. Qin, C.K., Majid, N.Z., Shamjuddin, A., Amin, N.A.S., Yussuf, M.A.M., Hassan, Z.H., Hamid, N.H.A., Zainan, N.H., Jaafar, N.R. (2025). Parametric optimization on acid hydrolysis of ozone pre-Treated oil palm empty fruit bunch for enhanced glucose production. *AIP Conference Proceedings*, 3225(1), 1–6. DOI: 10.1063/5.0267373.
- [37]. Baksi, S., Sarkar, U., Villa, R., Basu, D., Sengupta, D. (2023). Conversion of biomass to biofuels through sugar platform: A review of enzymatic hydrolysis highlighting the trade-off between product and substrate inhibitions. *Sustainable Energy Technologies and Assessments*, 55(September 2022) DOI: 10.1016/j.seta.2022.102963.
- [38]. Shiva, Rodríguez-Jasso, R.M., López-Sandin, I., Aguilar, M.A., López-Badillo, C.M., Ruiz, H.A. (2023). Intensification of enzymatic saccharification at high solid loading of pretreated agave bagasse at bioreactor scale. *Journal of Environmental Chemical Engineering*, 11(1), 109257. DOI: 10.1016/j.jece.2022.109257.
- [39]. Shah, S.R., Ishmael, U.C., Palliah, J.V., Asras, M.F.F., Ahmad, S.S.B.N.W. (2016). Optimization of the enzymatic saccharification process of empty fruit bunch pretreated with laccase enzyme. *BioResources*, 11(2), 5138–5154. DOI: 10.15376/biores.11.2.5138-5154.
- [40]. Yemis, O., Mazza, G. (2012). Optimization of furfural and 5-hydroxymethylfurfural production from wheat straw by a microwave-assisted process. *Bioresource Technology*. 109, 215–223. DOI: 10.1016/j.biortech.2012.01.031.
- [41]. Hu, Y., Priya, A., Chen, C., Liang, C., Wang, W., Wang, Q., Sze, C., Lin, K., Qi, W. (2023). Recent advances in substrate-enzyme interactions facilitating efficient biodegradation of lignocellulosic biomass: A review. *International Biodeterioration & Biodegradation*, 180, 105594. DOI: 10.1016/j.ibiod.2023.105594.
- [42]. Abd Majid, N.Z., Shamjuddin, A., Asli, U.A., Mohd Fauzi, N.A.F., Hussain, S.N., Masri, A.N., Zainan, N.H., Jaafar, N.R. (2025). Optimization of Temperature, Cellulase Concentration and pH value of Enzymatic Saccharification for Producing Sugar from Ozone Pre-treated Oil Palm Empty Fruit Bunch. *Bioprocessing and Biomass Technology*, 4(1), 33–37. DOI: 10.11113/bioprocessing.v4n1.73.
- [43]. Wang, Q., Chang, L., Wang, W., Hu, Y., Yue, J. (2023). Simultaneous saccharification of hemicellulose and cellulose of corncob in a one-pot system using catalysis of carbon based solid acid from lignosulfonate. *Royal Society of Chemistry*. 13, 28542–28549. DOI: 10.1039/d3ra05283d.
- [44]. Mutrakulcharoen, P., Pornwongthong, P. (2020). Inhibitory Effect of Inorganic Salts Residuals on Cellulase Kinetics in Biofuel Production from Lignocellulose Biomass. *2020 International Conference and Utility Exhibition on Energy, Environment and Climate Change (ICUE)*. DOI: 10.1109/ICUE49301.2020.9307055
- [45]. Singh, S., Agarwal, M., Bhatt, A., Goyal, A., Moholkar, V.S. (2015). Ultrasound enhanced enzymatic hydrolysis of *Parthenium hysterophorus*: A mechanistic investigation. *Bioresource Technology*, 192, 636–645. DOI: 10.1016/j.biortech.2015.06.031.
- [46]. Brown, J., Lindstrom, J.K., Ghosh, A., Rollag, S.A., Brown, R.C. (2024). Production of sugars from lignocellulosic biomass via biochemical and thermochemical routes. *Frontiers in Energy Research*, 12(February), 1–34. DOI: 10.3389/fenrg.2024.1347373.

- [47]. Ioelovich, M. (2015). Study of kinetics of enzymatic hydrolysis of cellulose materials. *ChemXpress*, 8(4), 231–239. DOI: 10.13140/RG.2.1.3185.6806.
- [48]. Wang, K., Shen, Z., Wang, X., Li, Z., Cheng, S. (2024). Advances in enhancing the enzymatic saccharification process of lignocellulosic biomasses for bioethanol production. *Biomass and Bioenergy*, 191, 107450. DOI: 10.1016/j.biombioe.2024.107450.
- [49]. Angeltveit, C.F., Várnai, A., Eijsink, V.G.H., Horn, S.J. (2024). Enhancing enzymatic saccharification yields of cellulose at high solid loadings by combining different LPMO activities. *Biotechnology for Biofuels and Bioproducts*, 17(1), 1–14. DOI: 10.1186/s13068-024-02485-6.